Morphology of CIGS thin films deposited by single-stage process and three-stage process at low temperature*

ZHANG Jia-wei (张嘉伟)[1,2], XUE Yu-ming (薛玉明)[1], LI Wei (李微)[2]**, ZHAO Yan-min (赵彦民)[2], and QIAO Zai-xiang (乔在祥)[2]**

1. Tianjin Key Laboratory of Film Electronic and Communication Devices, School of Electronics Information Engineering, Tianjin University of Technology, Tianjin 300384, China

2. National Key Laboratory of Power Sources, Tianjin Institute of Power Sources, Tianjin 300381, China

3. School of Science, Tianjin Polytechnic University, Tianjin 300381, China

(Received 19 July 2013; Revised 18 August 2013)

©Tianjin University of Technology and Springer-Verlag Berlin Heidelberg 2013

$Cu(In,Ga)Se_2$ (CIGS) thin films are prepared by a single-stage process and a three-stage process at low temperature in the co-evaporation equipment. The quite different morphologies of CIGS thin films deposited by two methods are characterized by scanning electron microscopy (SEM). The orientation of CIGS thin films is identified by X-ray diffraction (XRD) and Raman spectrum, respectively. Through analyzing the film-forming mechanisms of two preparation processes, we consider the cause of such differences is that the films deposited by three-stage process at low temperature evolve from Cu-poor to Cu-rich ones and then back to Cu-poor ones. The three-stage process at low temperature results in the CIGS thin films with the (220)/(204) preferred orientation, and the ordered vacancy compound (OVC) layer is formed on the surface of the film. This study has great significance to large-scale industrial production.

Document code: A **Article ID:** 1673-1905(2013)06-0449-5

DOI 10.1007/s11801-013-3130-3

For space applications, light weight $Cu(In,Ga)Se_2$ (CIGS) devices show the potential to increase the specific power with excellent radiation hardness[1,2]. In 2008, the American National Renewable Energy Laboratory (NREL) used three-stage process to deposit CIGS thin film solar cells on glass substrate, which yielded an efficiency of 19.9%[3]. In 2011, the German ZSW laboratory improved the efficiency of CIGS thin film solar cells on glass substrate to 20.3%[4]. The efficiency of flexible CIGS thin film solar cells on polyimide (PI) substrate prepared by Swiss Federal Institute of Technology reached 17.6% in 2010[5], and increased to 18.7% in 2012[6].

In this paper, CIGS absorber layers are deposited on PI substrate via a single-stage process and a three-stage process at low temperature in the co-evaporation equipment, respectively. The quite different morphologies of CIGS thin films are characterized by scanning electron microscopy (SEM), and the orientation of CIGS thin films is identified by X-ray diffraction (XRD) and Raman spectrum, respectively. This study has great significance to large-scale industrial production.

CIGS absorber layers were prepared in a co-evaporation equipment with Cu, In, Ga, Se evaporation sources at the base pressure of 1.0×10^{-4} Pa. The evaporation sources and substrate heating system were adjusted by proportional-integral-derivative (PID) temperature controller. The distance between evaporation sources and substrate is about 25–28 cm. CIGS thin films were deposited by a single-stage process and a three-stage process at low temperature.

In the single-stage process at low temperature, Cu, In, Ga and Se were deposited at the same time with the substrate temperature of 490 °C in 55 min as shown in Fig.1(a). In the three-stage process at low temperature as shown in Fig.1(b): Firstly, In, Ga and Se were deposited with the substrate temperature of 350 °C in 20 min to get a precursor layer with In:Ga=0.7:0.3. Secondly, Cu and Se were evaporated at the substrate temperature of 490 °C with constant power heating, and we utilized end-point detection method to control the preparing time[7]. Thirdly, In, Ga and Se were co-evaporated with substrate temperature of 490 °C in 3–5 min.

The thicknesses of CIGS thin films were tested by a KLA Tencor mechanic profiler, and the compositions were identified by a Spectro Xepos XRF. A Rigaku TTRⅢ XRD and a Horiba Tubin Yvon T4000 Raman spectrum were used to detect the orientation of the films. The surface and cross-section images were obtained by a Hitachi S-4800 SEM.

Fig.2 shows the SEM images for the CIGS thin films deposited by a single-stage process and a three-stage

* This work has been supported by the National High Technology Research and Development Program of China (No.2012AA050701).

** E-mails: orwell.x@163.com; wli@nklps.org

process at low temperature. Fig.2(a) and (b) present the surfaces of CIGS thin films, and it can be seen that the CIGS thin films deposited by single-stage process have a large number of triangular-shaped grains, and the structure is compact. But there are some small holes between the grains. However, the CIGS thin films prepared by three-stage process have a lot of block grains, and the structure is extremely dense. Practically, there is no hole between the grains. The cross-sectional structures of the CIGS thin films are revealed by Fig.2(c) and (d). It can be seen from Fig.2(c) that the grain size of CIGS thin films prepared by single-stage process is small. The grain size is large in the longitudinal direction, but in the transverse direction, the grain boundaries can be found obviously. Fig.2(d) shows the cross-sectional structure for the CIGS thin films deposited by three-stage process is very dense. There is no obvious boundary from both longitudinal and lateral views.

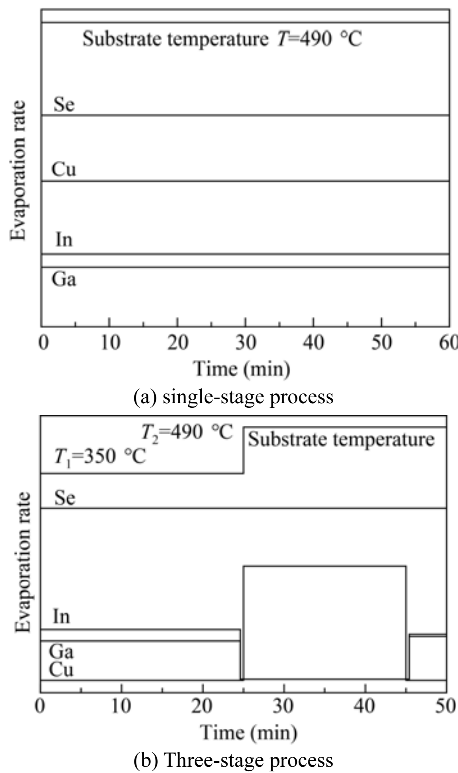

(a) single-stage process

(b) Three-stage process

Fig.1 Co-evaporation process diagrams of single-stage process and three-stage process at low temperature

It is shown that if the films are Cu-rich at the beginning of the growth, they are found to be (112) oriented, and the degree of this orientation increases as the Cu excess decreases[8,9]. In contrast, the films grown from a Cu-poor start are found to be (220)/(204) oriented[10]. Some researches have shown that for the commonly used three-stage process, the degree of (220)/(204) orientation depends on the Se flux in the first stage of the growth[11], while other orientations in the films are correlated with the properties of the Mo back contact[12]. In this paper, the CIGS thin films are deposited on the same Mo back and contacted with the same Se flux.

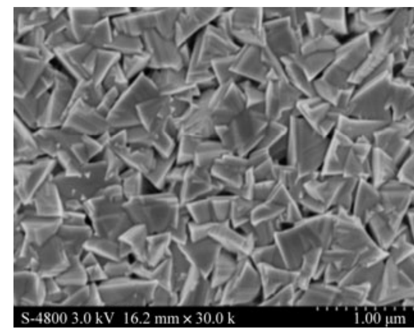

(a) Surface, single-stage process

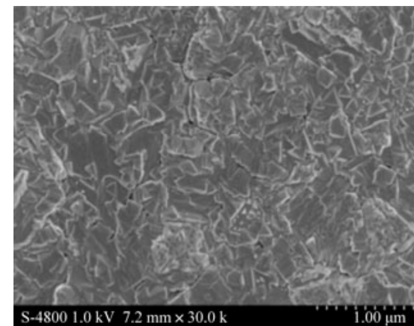

(b) Surface, three-stage process

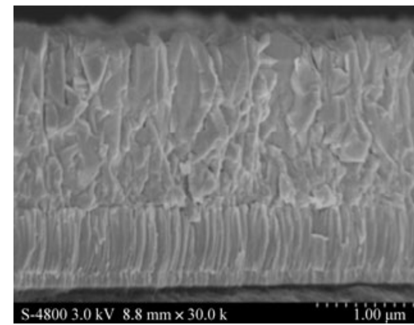

(c) Cross-sectional structure, single-stage process

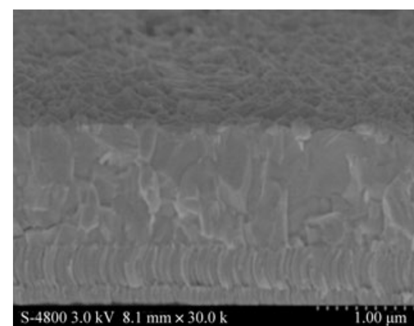

(d) Cross-sectional structure, three-stage process

Fig.2 The SEM images for the films deposited by single-stage and three-stage processes

Fig.3 shows the XRD patterns of the CIGS thin films prepared by two different processes, which have different crystal orientations. $Cu(In_{0.7}, Ga_{0.3})_2Se_3$ phase exists in both CIGS thin films which have two crystalline orientations: one is (112) crystal direction, and the other one is (220)/(204) crystal direction accompanied by (312) crystal orientation. The CIGS thin films deposited by single-stage process at low temperature have strong (112)

and (220)/(204) peaks, but there is no obvious preferred orientation. However, the CIGS thin films prepared by three-stage process at low temperature have a strong (220)/(204) peak which is the preferred orientation.

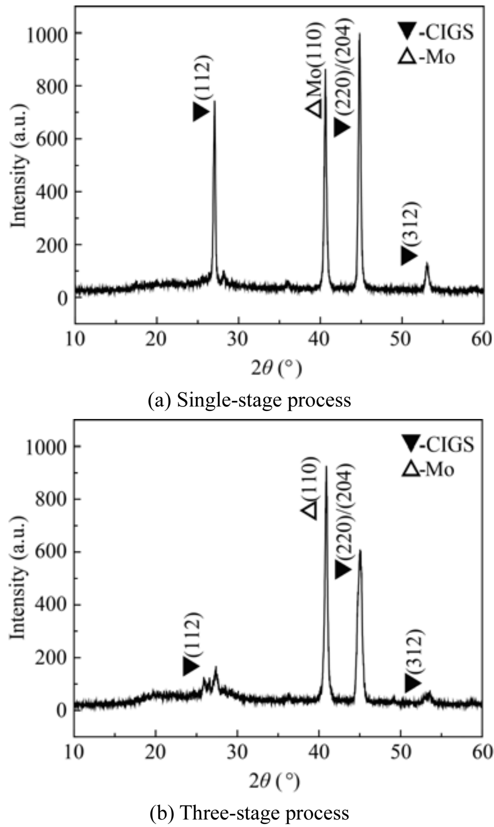

(a) Single-stage process

(b) Three-stage process

Fig.3 XRD patterns for the films deposited by different processes

We can see from Tab.1 that the compositions of CIGS thin films deposited by different processes are similar, but their morphologies and preferred orientations are quite different. We consider the cause of such differences is the different film-forming mechanisms. The three-stage process is more complicated than the single-stage process, and the films evolve from Cu-poor to Cu-rich ones and then back to Cu-poor ones as shown in Tab.2.

Tab.1 The compositions of CIGS thin films deposited by different processes

Porcess	Cu (%)	Ga (%)	Se (%)	In (%)	Cu/(In+Ga) (%)	Ga/(In+Ga) (%)
Single-stage	23.13	7.69	50.24	18.94	0.87	0.29
Three-stage	22.90	7.76	51.10	18.24	0.88	0.30

Tab.2 The compositions of CIGS thin films deposited by three-stage process at different stages

Stage	Cu (%)	Ga (%)	Se (%)	In (%)	Cu/(In+Ga) (%)	Ga/(In+Ga) (%)
1st stage	0.13	14.46	49.97	35.44	0.01	0.29
2nd stage	27.22	6.85	50.23	15.69	1.21	0.30
3rd stage	22.90	7.76	51.10	18.24	0.88	0.30

In the second stage, the $(In,Ga)_2Se_3$ precursor layers transform to $Cu(In,Ga)Se_2$ by exposing to fluxes of Cu and Se at the substrate temperature of 490 °C until the overall composition becomes Cu-rich. Tab.2 demonstrates the composition of CIGS thin films at the end of the second stage.

During the second stage of the growth, the top surface of films is grown more Cu-rich than the bulk, and we believe that this Cu gradient results in a Cu diffusion which acts as a driving force for the recrystallization of the film[10]. The SEM images for the CIGS thin films are presented in Fig.4, and we can see that the grains of thin films are large with few boundaries, but there is a layered structure at the surface of thin films. The Raman spectrum for the films deposited at the end of the second stage is shown in Fig.5, which indicates that Cu_xSe can be locally presented at the surface of the films. The spectrum shows the presence of the Cu_xSe-related peak at about 155 cm^{-1} for CIGS thin films at the end of the second stage. It is the fact that Cu-rich CIGS is a two-phase mixture ($Cu(In,Ga)Se_2$ and Cu_xSe), where the chief part of Cu_xSe phase can swim on top of $Cu(In,Ga)Se_2$ in most processes. The emissivity of Cu_xSe is higher than that of stoichiometric or Cu-poor CIGS. During a deposition process, the substrate temperature is recorded while the heating power of substrate remains constant ("constant power mode"), and crossing the "stoichiometry line" from Cu-poor to Cu-rich manifests itself by a temperature drop[7,13]. When the substrate temperature is higher than 523 °C, the Cu_xSe turns into liquid phase which accelerates the CIGS grain growth rate, while the In_{Cu}, Ga_{Cu} and V_{Cu} defects which exist in the original film all disappear due to Cu-rich structure[14-17]. Recently, Barreau[18] proposed that the liquid phase Cu_xSe was not the necessary condition to deposit large grain CIGS thin films. The experiments also confirmed that the CIGS thin film which did not undergo a Cu_xSe liquid phase stage could also get a large grain size[19]. In this paper, the substrate temperature is too low to generate liquid phase Cu_xSe on the surface of CIGS, but the Cu-poor/rich/poor sequence still promotes the grains to be large.

However, the CIGS thin films deposited by single-stage process do not have the Cu-poor/rich/poor sequence. As we can see from Tab.3, the compositions maintain constant, and the films do not present a transformation from Cu-poor to Cu-rich ones and then back to Cu-poor ones.

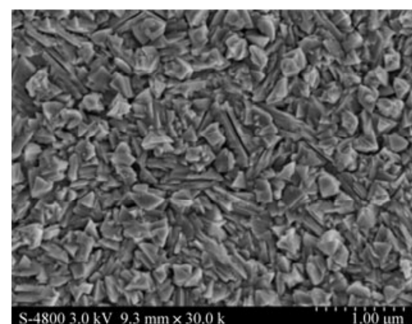

(a) Surface

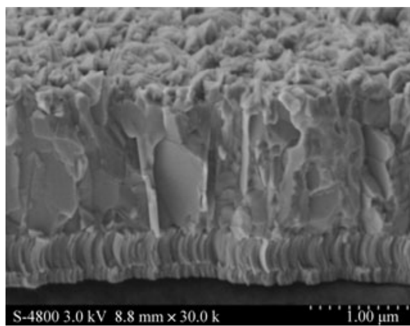

(b) Cross-sectional structure

Fig.4 The SEM images for the films deposited at the end of the second stage

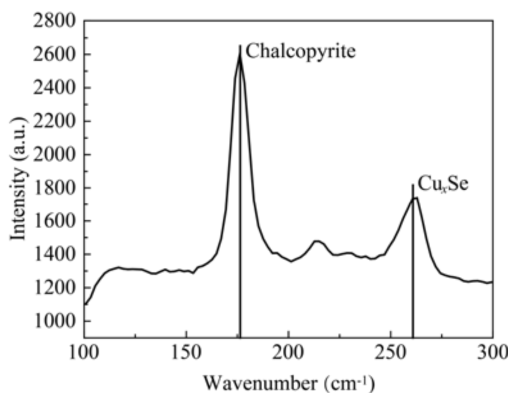

Fig.5 The Raman spectrum for the films deposited at the end of the second stage

Tab.3 The compositions of CIGS thin films with different preparing time by single-stage process at low temperature

Time	Cu (%)	Ga (%)	Se (%)	In (%)	Cu/(In+Ga) (%)	Ga/(In+Ga) (%)
20 min	23.13	7.69	50.24	18.94	0.87	0.29
30 min	22.89	8.06	50.41	18.03	0.86	0.30
40 min	23.35	8.09	50.78	17.77	0.90	0.31
50 min	23.55	7.74	50.71	17.99	0.91	0.30

Fig.6 shows the XRD patterns for the CIGS thin films deposited by single-stage process at low temperature with different preparing time. There are two crystalline orientations: one is the (112) crystal direction, and the other one is (220)/(204) orientation.

The two different processes can influence the composition and phase formation of the CIGS films. The Raman spectra of the CIGS thin films grown with different processes are shown in Fig.7. The spectra show that the OVC-related peak appears at about 155 cm^{-1} for CIGS thin films deposited by three-stage process, but does not appear for those deposited by single-stage process. We assume that the CIGS thin films grown with a Cu-poor /rich/poor sequence make the presence of OVC phase.

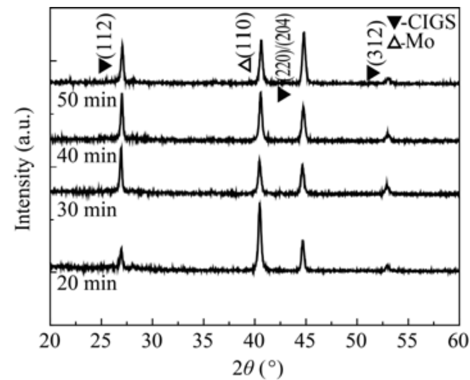

Fig.6 The XRD patterns for the films deposited by single-stage process at low temperature with different preparing time

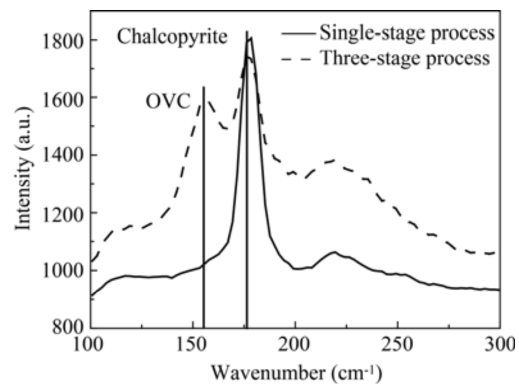

Fig.7 The Raman spectra for the films deposited by two different processes

CIGS thin films grown by a single-stage process and a three-stage process are investigated. The quite different morphologies of CIGS thin films deposited by two methods are characterized by SEM. The grains grown by three-stage process are much larger than those deposited by single-stage process. The orientation of CIGS thin films is identified by XRD and Raman spectrum, respectively. The Raman spectra show that there is an OVC-related peak at about 155 cm^{-1} for CIGS thin films deposited by three-stage process, but there is not for those deposited by single-stage process. Through analyzing the film-forming mechanisms of two preparation processes, the reason of such differences is that the films deposited by three-stage process at low temperature evolve from Cu-poor to Cu-rich ones and then back to Cu-poor ones. The CIGS thin films deposited by the three-stage process at low temperature have the (220)/(204) preferred orientation, and there is an OVC layer on the surface of the film. The study has great significance to large-scale industrial production.

References

[1] R. Zwanenburg and M. Kroon, Requirements for Thin Film Solar Arrays and the Development Status of a New Solar Cell Blanker Concept, Proc. Seventh European

Space Power Conference, 2005.

[2] R. M. Burgess, W. E. Devaney and W. S. Chen, Peroramnce Analysis of $CuInSe_2$ and GaAs Solar Cells Aboard the LIPS-III Flight Boeing Lightweight Panel, 23rd IEEE Photovoltaic Specialists Conference, 1465 (1993).

[3] Ingrid Repins, Miguel A. Contreras, Brian Egaas, Clay Dehart, John Scharf, Craig L Perkins, Bobby To and Rommel Noufi, Prog. Photovolt: Res. Appl. **16**, 235 (2008).

[4] Philip Jackson, Dimitrios Hariskos, Erwin Lotter, Stefan Paetel, Roland Wuerz, Richard Menner, Wiltraud Wischmann and Michael Powalla, Progress in Photovoltaics: Research and Applications **19**, 894 (2011).

[5] A. Chirilă, D. Guettler, P. Bloesch, S. Nishiwaki, S. Seyrling, S. Buecheler, R. Verma, F. Pianezzi, Y. E. Romanyuk, G. Bilger, R. Ziltener, D. Bremaud and A. N. Tiwari, Optimization of Composition Grading in $Cu(In,Ga)Se_2$ for Flexible Solar Cells and Modules, 35th IEEE Photovoltaic Specialists Conference, 656 (2010).

[6] A. Chirilă, S. Buecheler, F. Pianezzi, P. Bloesch, C. Gretener, A. R. Uhl, C. Fella, L. Kranz, J. Perrenoud, S. Seyrling, R. Verma, S. Nishiwaki, Y. E. Romanyuk, G. Bilger and A. N. Tiwari, Nature Materials **10**, 857 (2011).

[7] M. A. Contreras, J. Tuttle, A. Tennant, K. Ramanathan, S. Asher, A. Franz, J. Keane, L. Wang and R. Noufi, Solar Energy Materials & Solar Cells **41-42**, 231 (1996).

[8] J. Kessler, J. Scholdstrom and L. Stolt, Analysis of CIGS Films and Devices Resulting from Different Cu-rich to Cu-poor Transitions, Proceedings of 17th European Photovoltaic Solar Energy Conference, Munich, 1019 (2001).

[9] Li Bo-yan, Zhang Yi, Liu Wei and Sun Yun, Optoelectronics Letters **8**, 348 (2012).

[10] J. Kessler, C. Chityuttakan, J. Lu, J. Scholdstrom and L. Stolt, Prog. Photovolt: Res. Appl. **11**, 319 (2003).

[11] Chaisitsak S., Tokita Y., Miyazaki H., Mikami R., Yamada A. and Konagai M., Control and Preferred Orientation for $Cu(In,Ga)Se_2$ Thin Films and Its Effect on Solar Cell Performance, Proceedings of 17th European Photovoltaic Solar Energy Conference, Munich, 1011 (2001).

[12] M. A. Contreras, B. Egaas, D. King, A. Swartzlandera and T. Dullweberb, Thin Solid Films **361-362**, 167 (2000).

[13] N. Kohara, T. Negami, M. Nishitani and T. Wada, Jpn. J. Appl. Phys. **34**, L1141 (1995).

[14] Xue Yu-ming, Xu Chuan-ming, Zhang Li, Sun Yun, Wang Wei and Yang Bao-he, Journal of Optoelectronics·Laser **19**, 348 (2008). (in Chinese)

[15] Lin Z., Xu F. and Weaver J. H., Phys. Rev. B **36**, 5777 (1987).

[16] D. S. Albin, G. D. Mooney, A. Duda, J. Tuttle, R. Matson and R. Noufi, Solar Cells **30**, 47 (1991).

[17] Xin Zhi-jun, Chen Xi-ming, Qiao Zai-xiang, Wang He, Xue Yu-ming, Pan Zhen and Tian Yuan, Oproelectronics Letters **9**, 112 (2013).

[18] N. Barreau, T. Painchaud, F. Couzinié-Devy, L. Arzel and J. Kessler, Acta Materialia **58**, 5572 (2010).

[19] T. Nakada, H. Ohbo, M. Fukuda and A. Kunioka, Solar Energy Materials and Solar Cells **49**, 261 (1997).